PHYSICAL REVIEW B VOLUME 8, NUMBER 5 1 SEPTEMBER 1973

Inelastic-Neutron-Scattering Study of Acoustic Phonons in Nb_3Sn†

J. D. Axe and G. Shirane
Brookhaven National Laboratory, Upton, New York 11973
(Received 21 February 1973)

Transverse-acoustic-phonon frequencies and line shapes have been studied as a function of temperature in Nb_3Sn. There is a substantial ($\sim 10\%$) reduction in all of the mode frequencies studied between 300 °K and the cubic-tetragonal transformation temperature $T_M = 45$ °K. Even more pronounced elastic softening is observed for $[\zeta\zeta 0]T_1$ phonons with $q \lesssim q_{\text{Z.B.}}/10$. As $T \to T_M$ from above, phonons in this latter group acquire an unusual quasielastic "central" component in addition to the phononlike sidebands. The evolution of this central component is adequately described by a phenomenological theory which assumes an additional low-frequency ralaxation mechanism for the acoustic phonons. Finally, abrupt changes in certain phonon lifetimes are detected near the superconducting transformation temperature $T_c = 18.0$ °K. This behavior is traced to the the inability of phonons with energies less than that of the superconducting gap $2\Delta(T)$ to decay by creation of excited electron-quasiparticle pairs. These measurements give an estimate of $2\Delta(0) = (4.4 \pm 0.6)k_B T_c$ and reveal a strong anisotropy in the electron–transverse-phonon interaction.

I. INTRODUCTION

Very high superconducting transformation temperatures occur in many binary or pseudobinary compounds of the β-tungsten structure.[1] This fact, coupled especially with the occurrence among these same materials of structural phase transformations known to involve lattice vibrational instabilities,[2–7] has created a lively interest in the lattice dynamics and in particularly the nature of electron-phonon interaction in materials with this structure. Very rewarding in this respect have been experimental studies of the temperature dependent elastic properties which have revealed in V_3Si[3] and Nb_3Sn[4,8–10] a shear wave whose velocity nearly vanishes at the structural transformation temperature T_M. This elastic instability is thought to result from what has been called a band Jahn-Teller (JT) effect. The basic idea, first proposed by Labbé and Friedel[11] and since elaborated by various authors,[12–16] is that one is dealing with a nearly empty set of d-electron bands whose degeneracy is removed by the elastic strain. The re-equilibration of the electrons within the split bands of the strained structure can in favorable conditions balance the normal increase in elastic energy. This destabilizing d-electron contribution is one, however, which increases with decreasing temperature as the Fermi surface becomes sharper.

Experimental information bearing upon the lattice dynamics of these compounds has been chiefly limited to that available from elastic-constant and specific-heat measurements.[17,18] However, a recent inelastic-neutron-scattering study of V_3Si was performed which established that the elastic softening associated with the phase transformation extends, though to a lesser degree, over a significant region of the Brillouin zone.[19] These experiments were made difficult owing to the fact that the vanadium nucleus has an extremely unfavorable ratio of the coherent to incoherent scattering cross section.

From the point of view of nuclear properties Nb_3Sn is much more favorable for neutron investigations, but single crystals of a size sufficient for a thorough inelastic scattering investigation are not available. However, a recent study[20] of the elastic neutron scattering has revealed previously undetected "forbidden" Bragg reflections (see Fig. 1) resulting from Nb-sublattice distortions in the tetragonal phase. The full implication of this distortion, and the linear piezo-optic coupling[20,21] from which it arises, on the superconducting properties of Nb_3Sn have yet to be fully explored.

The present investigation extends to much shorter wavelengths the study of the elastic instability near $T_M \cong 45$ °K in Nb_3Sn using inelastic neutron scattering. In addition the phonon dispersion relations were measured in as many other branches as the small sample volume would permit. These general results are presented in Sec. II. Two very interesting and rather unique phenomena discovered in the course of this investigation are singled out for further study in Secs. III and IV. A preliminary account of the first of these, having to do with unusual phonon line shapes in the soft TA branch at temperature near T_M has already appeared.[22] Section IV is devoted to a description of phonon linewidth changes with temperature in the vicinity of the superconducting transformation temperature $T_c = 18.0$ °K and which have direct bearing on the electron-phonon interaction parameters of most importance in understanding the superconductivity in Nb_3Sn.

II. ACOUSTIC PHONON DISPERSION

The experiments to be described were carried out on a triple axis spectrometer at the Brookhaven

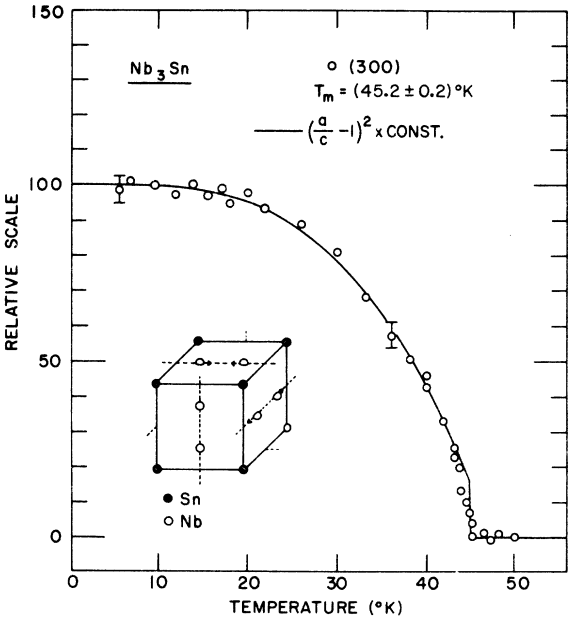

FIG. 1. Comparison of the intensity of the "forbidden" (300) reflection in Nb_3Sn with the square of the tetragonal order parameter $[(a/c)-1]$. The insert shows the nature of the Nb-sublattice distortion which produces this reflection and which accompanies the tetragonal distortion of the unit cell.

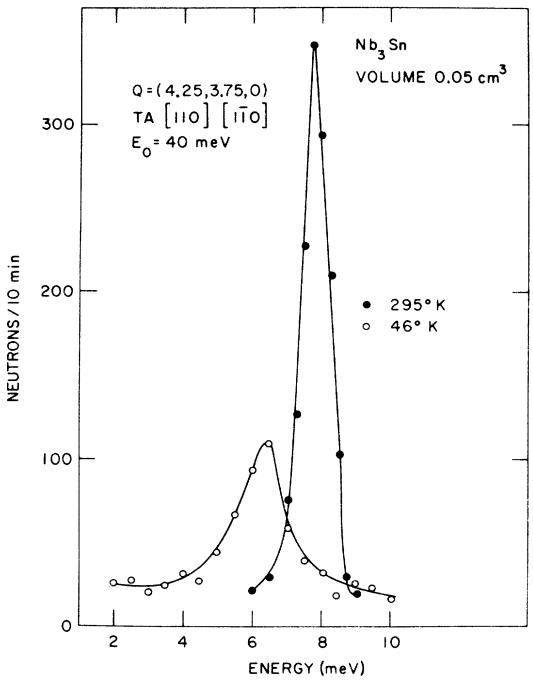

FIG. 2. Representative inelastic neutron scattering peaks from $[\zeta\zeta 0]T_1$ phonons in Nb_3Sn at room temperature and just above the structural transformation temperature $T_M = 45$ °K. The cubic reciprocal-lattice vector $a^* = (2\pi/a) = 1.189$ Å^{-1} at 46 °K.

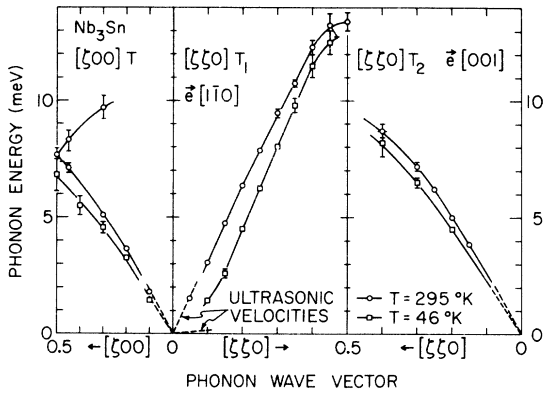

FIG. 3. Dispersion relations for transverse acoustic phonons in Nb_3Sn at two temperatures. The ultrasonic velocities are taken from Rehwald *et al.* (Ref. 8).

high-flux beam reactor. The Nb_3Sn crystal grown by Hanak and Berman[23] was the same sample used in our previous study. Although of excellent quality (mosaic spread $< 0.10°$ in cubic phase), the sample volume (~ 0.05 cm^3) is indeed quite small to attempt inelastic-neutron-scattering studies. As a result our measurements were limited to the lower-energy portion ($\lesssim 20$ meV) of the phonon spectrum. Even this range of energy transfer would have been impossible to investigate without the use of highly efficient vertically focusing pyrolytic-graphite monochromating crystals, used wherever possible in conjunction with pyrolytic graphite filters.[24] Some care was also necessary to adjust the incident neutron energy (between 5 and 45 meV) and other instrumental parameters to achieve an acceptable compromise between resolution and intensity. While much more could undoubtedly have been accomplished with a larger sample in the way of detailed quantitative results, the present experiments were very rich in terms of novel phenomena.

An example of the quality of the phonon data which was obtained under somewhat better than average conditions is shown in Fig. 2. These phonons lie along $\vec{q} = [\zeta\zeta 0]$ with eigenvectors $\vec{e}$ along $[\zeta\bar{\zeta}0]$ in the limit $\zeta \to 0$. These T_1 modes have a velocity proportional to $(C_{11} - C_{12})^{1/2}$ and it is this combination of elastic constants which softens and nearly vanishes at the transformation temperature T_M.[4,8,9] As was observed in V_3Si, there is an appreciable shift of the T_1 phonon frequencies with temperature even at quite substantial values of q. Data taken at room temperature and at T_M for transverse acoustic modes along $[\zeta 00]$ and $[\zeta\zeta 0]$ are summarized in Fig. 3 and Table I. At room temperature all the neutron data fits smoothly with extrapolations of the ultrasonic velocities.[8] *All* of the mode frequencies measured soften as the temperature is lowered, contrary to the slight stiffening that most materials experience on cooling.

TABLE I. Nb_3Sn acoustic phonon energies (meV).

	$[\zeta 00]T$		$[\zeta\zeta 0]T_1$		$[\zeta\zeta 0]T_2$	
ζ	46 °K	295 °K	46 °K	295 °K	46 °K	295 °K
0.05	•••	•••	•••	1.52 ± 0.07	•••	•••
0.1	1.45 ± 0.05	1.79 ± 0.05	•••	3.07 ± 0.05	•••	•••
0.15	•••	•••	2.6 ± 0.2	4.75 ± 0.05	3.85 ± 0.15	•••
0.2	3.26 ± 0.1	3.65 ± 0.1	4.49 ± 0.1	6.35 ± 0.12	5.00 ± 0.1	4.50 ± 0.1
0.25	•••	•••	6.23 ± 0.1	7.85 ± 0.15	6.22 ± 0.2	•••
0.3	4.55 ± 0.25	5.10 ± 0.1	8.03 ± 0.1	9.45 ± 0.25	7.18 ± 0.2	6.5 ± 0.2
0.35	•••	•••	9.8 ± 0.3	10.75 ± 0.2	•••	•••
0.4	5.5 ± 0.4	•••	11.5 ± 0.5	12.3 ± 0.3	8.70 ± 0.3	8.2 ± 0.5
0.45	•••	7.1 ± 0.2	12.5 ± 0.5	13.5 ± 0.35	•••	•••
0.5	6.8 ± 0.8	7.65 ± 0.3	•••	13.4 ± 0.4	•••	•••

The most striking feature of Fig. 3 however is that for $[\zeta\zeta 0]T_1$ phonons, the neutron data with $\zeta \gtrsim 0.1$ apparently now bears little relation to the extrapolated ultrasonic velocity. Further, higher resolution measurements were therefore made to determine the nature of the dispersion in this region ($\vec{q} \| [\zeta\zeta 0]$, $\zeta \leq 0.1$). (In the previous study on V_3Si, [19] this most interesting region was inaccessible to measurement because of the overwhelming elastic incoherent background scattering.) Some of these measurements are summarized in Fig. 4. It is apparent from Fig. 4 that there is no difficulty in establishing a linear extrapolation of the $\omega(q)$ data at small q to $q = 0$, at least at temperatures greater than ~ 55 °K. At lower temperatures, lineshape anomalies introduce some complications (see Sec. III and Fig. 6).

According to the existing band JT theory the elastic instability in Nb_3Sn is the result of interactions specifically involving the nearly empty d-electron bands. In the Migdal approximation the dispersion of the acoustic phonons at small q is of the form[16,25]

$$\omega_{ac}^2(\vec{q}) = \left(v(\vec{q})^2 + \sum_i A_i(\vec{q})\Pi_i(\vec{q})\right)q^2 , \quad (1)$$

with

$$\Pi_i(\vec{q}) = \sum_k \left(\frac{f_i(\vec{k}+\vec{q}) - f_i(\vec{k})}{\epsilon_i(\vec{k}+\vec{q}) - \epsilon_i(\vec{k})}\right). \quad (2)$$

$A_i(\vec{q})\Pi_i(\vec{q})$ is the contribution of the nearly empty d bands to the elastic stiffness and $v^2(\vec{q})$ are all of the remaining contributions which are assumed to be temperature independent. $\epsilon_i(\vec{k})$ and $f_i(\vec{k})$ are, respectively, the energy and the Fermi occupation factor of the kth state in the ith d subband. A characteristic feature of calculations based on Eq. (1) is the appearance of a change of slope or perhaps a stronger singularity in the phonon dispersion for phonon wave vectors which span parallel regions of the Fermi surface.[26] In fact, as Barisic[27] has emphasized, the JT theory of the transformation, the long-wavelength acoustic instability can be thought of as arising from such a Kohn-like anomaly at a small but finite wave vector. It is thus tempting to associate the wave vector at which the temperature-dependent change in slope shown in Fig. 4 with a linear dimension of the Fermi surface. (The value of $2k_F$ given is that appropriate to a linear band structure. For a spherical Fermi surface $2k_F$ would be larger by $\sqrt{2}$. More general Fermi surfaces are not uniquely defined by a single linear dimension.) Schuster has calculated phonon dispersion for V_3Si based on Eq. (1) which are qualitatively very similar to those of Fig. 4. The exact shape of the phonon dispersion depends of course on the assumed form of the d subbands $\epsilon_i(\vec{k})$, a point

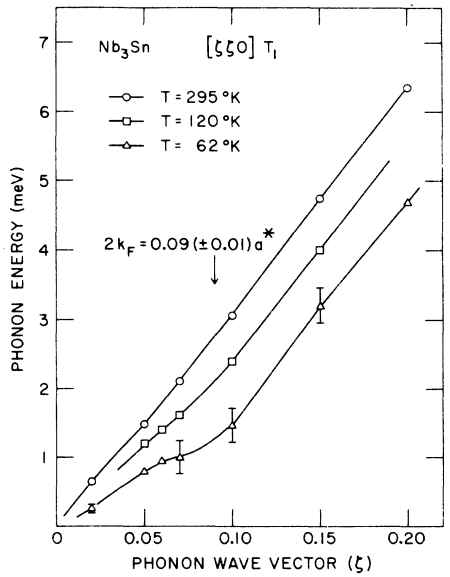

FIG. 4. $[\zeta\zeta 0]T_1$ phonon dispersion at small wave vector for three temperatures. The kink which appears at low temperatures may perhaps be understood as a Kohn anomaly which is in turn closely related to the elastic instability.

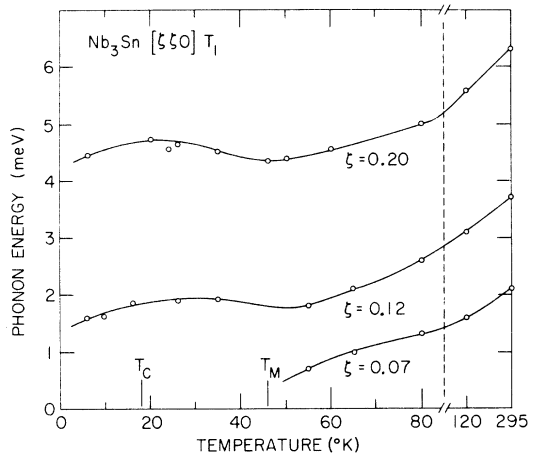

FIG. 5. Temperature dependence of selected $[\zeta\zeta 0]T_1$ phonons both above and below the cubic-tetragonal transformation temperature. The frequency renormalization below T_M is much less than that predicted by extrapolation of ultrasonic velocities.

which is presently not settled.[28]

It must however also be noted that a rigorous justification of the interpretation of the origin of the phonon dispersion in terms of q-dependent screening is not possible at this time. The difficulties in interpretation arise from the possible importance of *interband* scattering effects and the observation (see Sec. III) of sizable frequence dependent self-energy terms not considered in Eqs. (1) and (2). Neither for that matter do these equations [with $v(\vec{q})$ independent of temperature] explain the very noticeable softening of very-short-wavelength phonons ($q \gg 2k_F$) which occurs not only for the "soft" $[\zeta\zeta 0]T_1$ modes but as well for all branches investigated.

Below T_M the sample is composed of interspersed domains of tetragonal material with the tetragonal axis along one or another of the original cubic axes, and this added complication caused us to concentrate most extensively on measurements above T_M. Nonetheless, the temperature dependence of the principal TA modes below T_M was explored briefly, with the results shown in Fig. 5. More detailed measurements taken in the vicinity of the superconducting transformation temperature T_c will be presented in Sec. IV. Since no doubling or unusual asymmetries were observed to develop in the phonon line shapes below T_M (intensity arguments assure no components were missed entirely), the frequencies are taken to be the appropriately domain-averaged quantities. Above T_M well-resolved $[\zeta\zeta 0]T_1$ phonons were observed with ζ as small as 0.02. At all temperatures below T_M only very broad scattering centered at $\omega = 0$ could be observed for $\zeta \lesssim 0.1$. For $\zeta \gtrsim 0.1$, well-resolved $[110]T_1$ phonons were observed but the frequencies were considerably smaller than that predicted from extrapolation of ultrasonic velocities.[8] The dispersion in $\omega(q)$ at small q is very different for $T > T_M$ and $T < T_M$. Extrapolated ultrasonic velocities overestimate the $[\zeta\zeta 0]T_1$ softness for $T > T_M$, but the reverse is true for $T < T_M$.

III. CRITICAL NEUTRON SCATTERING

Now we turn our attention to the neutron scattering from the soft $[\zeta\zeta 0]T_1$ phonon branch with small wave vectors. For $\zeta \lesssim 0.1$, very unusual and interesting changes occur in the phonon line shapes as the temperature approaches T_M from above.[22] Typical of these observations are the data in Fig. 6 showing that as the temperature is lowered there is a gradual evolution of a central component in the scattering spectrum in addition to the familiar "phononlike" sidebands. Although the sideband structure continues to move to lower frequencies as the temperature is lowered, far more dramatic (note the logarithmic scale) is the growth of intensity of the central component which completely dominates the fluctuation spectrum near T_M. The apparent width of the central component can be essentially accounted for by the resolution of the instrument alone. Thus the intrinsic width which adds in quadrature to the instrumental width is very small, $\frac{1}{3}$ or less of the observed width. Figure 7 demonstrates that this central peak intensity maximizes at or very near T_M and thus represents the major contribution to the critical scattering associated with the structural transformation. Rehwald *et al.*[8] have stressed the possibility that the transformation occurs slowly over a range of ~7 °K in order to explain certain features of their ultrasonic results. Included for comparison in Fig. 7 is the (300) Bragg intensity, which is proportional to the square of the tetragonal distortion. At $T > T_M$, the intensity falls to a background level $\leq 0.5\%$ of the low-temperature Bragg intensity. This places a very low limit on the possible amount of transformed material present in our sample above 45 °K. In particular, the gradual growth of the central component in the critical scattering above T_M cannot be interpreted as arising somehow from already transformed regions of an inhomogeneous sample. Figure 8 shows that of the modes propagating in a {100} plane only those with propagation vectors nearly along the "soft" [110] direction have an appreciable central component.

The presence of a similar "extra" central peak in the critical fluctuations in displacive transformations in $SrTiO_3$ and $KMnF_3$ have recently been reported.[29,30] In all of these materials the phenomena observed bear a close qualitative resemblance to the divergent central Rayleigh peak which appears in the critical scattering of fluids. As is well known, in this case the central peak results

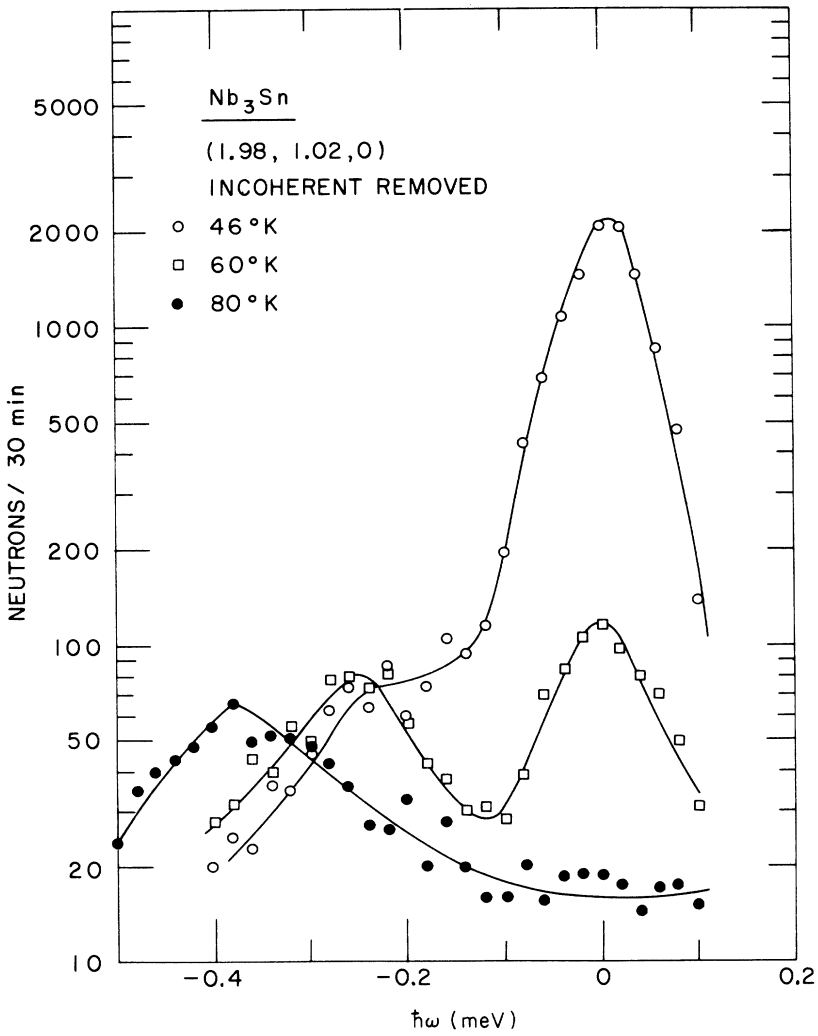

FIG. 6. Observed spectral profiles of $[\zeta\zeta 0]T_1$ phonon mode in Nb_3Sn with $\zeta = 0.02a^*$ at several temperatures above T_M. Only the phonon annihilation portion of the spectrum is shown. The data were taken with an incoming neutron energy of 5 meV and the energy resolution is ~0.1 meV.

from a linear coupling of adiabatic pressure fluctuations (the bare phonons) to thermal energy (i.e., entropy) fluctuations. On closer examination it is found that for the displacive transformations the coupling constant is proportional to $(d\eta/dT)^2$, where η is the appropriate order parameter for the transformation. Thus although this mechanism can be expected to contribute to a central component in the ordered state it must vanish above the ordering temperature where $\eta = 0$ independent of T. There exists however alternate interaction mechanisms which can give rise to similar modification of the low-frequency behavior of the fluctuation spectrum.[31] For example, Mountain[32] has shown how a similar central mode can arise from a coupling of the pressure fluctuations to the internal degrees of freedom of a nonsimple fluid.

One specific mechanism for similar structure in the phonon spectra of solids near phase transformations was suggested by Cowley[33] and has its origin in the difference between the collision-free and collision-dominated response of a phonon system. Although Cowley proposed the idea in connection with an optical-phonon-mode instability it is easily adaptable to the present case. Briefly, the physical idea is as follows: The strains associated with a given (long-wavelength) phonon mode produce through anharmonic terms in the lattice potential energy a time- and spatial-dependent modulation of the frequencies of the remaining (higher-frequency) thermal phonons. This frequency modulation gives rise to corresponding time-space modulation of the occupation number $n_{\text{th}}(\vec{r}, t)$ of the thermal phonons about an average value $\bar{n}_{\text{th}}$, the equilibrium value in a state of zero strain at the ambient bath temperature. If the frequency ω at which the long-wavelength strain varies is large compared to τ_{th}^{-1}, the inverse lifetime of the thermal phonon, this thermal disequilibrium $(n_{\text{th}} - \bar{n}_{\text{th}}$ has no time to relax and the energy involved in its establishment contributes to the "stiffness" of the long-wavelength strain. The long-wavelength

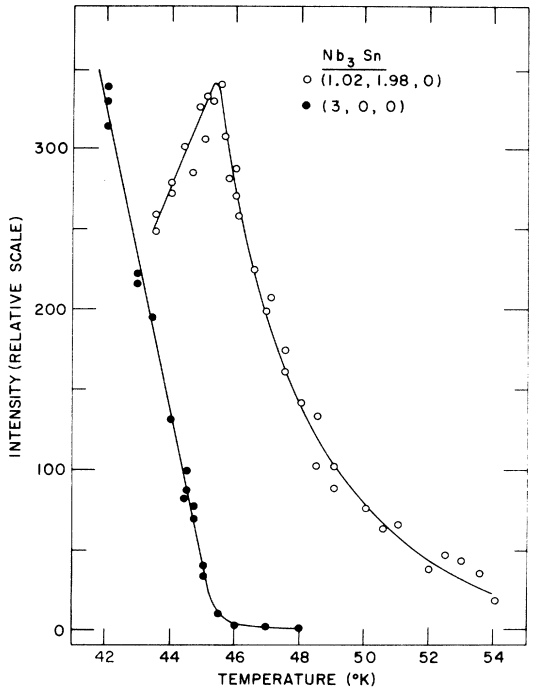

FIG. 7. Closed circles show the onset of the structural phase transformation as monitored by the "forbidden" (300) Bragg reflection. The open circles represent the temperature dependence of the central component in the neutron critical scattering spectrum.

phonon propagates in a collision-free (or zero-sound) regime. In the opposite limit $\omega \ll \tau_{th}^{-1}$, the thermal phonons have sufficient time within a cycle to relax to an equilibrium distribution specified by a local temperature, in the process reducing slightly the energy necessary to produce a given state of strain. The elastic stiffness is thus reduced in this collision dominated or hydrodynamic regime, but in the relaxation process some of the strain energy is now irreversibly lost to the thermal phonon system, providing an additional damping mechanism for the long-wavelength strain mode.

In order to see how the above considerations modify phonon line shapes in a neutron scattering experiment we note that the one phonon scattering probability for energy transfer $\hbar\omega$ and momentum transfer $\hbar Q$ is given by

$$S_\mu(Q,\omega) = |F_\mu(Q)|^2 [1+n(\omega)] A_\mu(\omega) , \tag{3}$$

where $\mu = (qj)$ is used to specify both the wave vector and branch index of a given mode, and $F_\mu(Q)$ is an inelastic structure factor. The phonon wave vector is reduced to the first Brillouin zone, i.e., $\vec{q} = \vec{Q} - \vec{G}$, where $\vec{G}$ is a reciprocal-lattice vector. The phonon dynamics are described by $A_\mu(\omega)$, the spectral correlation function which rather generally can be written in the form[34]

$$A_\mu(\omega) = (1/\pi)\mathrm{Im}[\Omega_\mu^2 - \omega^2 + \Pi_\mu^{an}(\omega)]^{-1} . \tag{4}$$

Ω_μ is the harmonic frequency of the mode. In the collision-free frequency regime if the anharmonic-phonon part of the self-energy function $\Pi_\mu^{an}(\omega)$ does not have sharply peaked structure at frequencies around Ω_μ it can often be satisfactorily represented in $A_\mu(\omega)$ by

$$\Pi_\mu^{an}(\omega) = \Delta_\mu^0 + i\omega\Gamma_\mu^0 , \tag{5}$$

Δ_μ^0 and Γ_μ^0 being frequency-independent constants. This gives rise to the familiar viscously damped classical oscillator response with a characteristic "quasiharmonic" frequency $\omega_\infty(\mu)$ given by

$$\omega_\infty^2(\mu) = \Omega_\mu^2 + \Delta_\mu^0 . \tag{6}$$

We wish to go beyond this and introduce in a phenomenological way the changes discussed above which occur as the frequency ω is lowered into the collision dominated regime.

Δ_μ and Γ_μ must vary with frequency in a way consistent with casuality. A simple modification of Eq. (5) which guarantees plausible behavior is

$$\Delta_\mu(\omega) = \Delta_\mu^0 - \delta_\mu^2 [\gamma_\mu^2/(\omega^2+\gamma_\mu^2)] , \tag{7}$$

$$\Gamma_\mu(\omega) = \Gamma_\mu^0 + \delta_\mu^2 [\gamma_\mu/(\omega^2+\gamma_\mu^2)] . \tag{8}$$

(In the following the mode index μ will be sup-

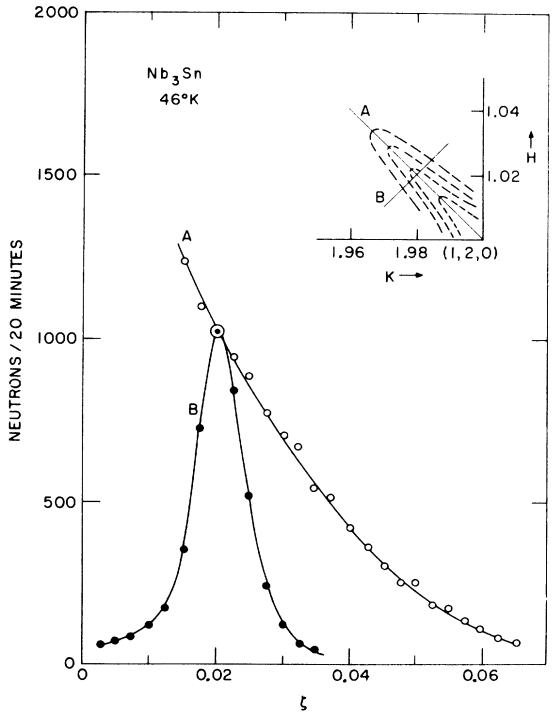

FIG. 8. Transverse and longitudinal scans of the central scattering component in the (100) plane. The abscissa shows the value of ζ for $[\zeta\zeta 0]$ of both A and B type.

pressed unless necessary.) For frequencies $\omega \ll \gamma$ the characteristic restoring force for the mode is shifted from its high frequency value ω_∞^2 to a lower value ω_0^2 given by

$$\omega_0^2 = \omega_\infty^2 - \delta^2 \ . \tag{9}$$

For small wave vector q we can identify $v_0 = \omega_0/q$ and $v_\infty = \omega_\infty$ as the velocity of (hydrodynamic) first sound and (high-frequency) zero sound, respectively.

A rigorous theoretical discussion of lattice dynamics valid in both first- and zero-sound regimes is quite complicated.[35] However, in the Appendix we sketch the derivation of a simple interpolation formula for the phonon self-energy connecting the two frequency regimes using a single relaxation-time approximation. It exposes some of the feature which would be present in a more serious calculation and at the same time provides a microscopic basis for the parameters δ and γ introduced above. It is however only a very limited theoretical justification of Eq. (7) and (8) which we continue to regard as primarily phenomenological in origin.

In order to see how the low frequency structure in $\Pi^{an}(\omega)$ is reflected in $S(Q, \omega)$ it is convenient to assume that (i) $(\delta^2/\gamma) \gg \Gamma_0$ and (ii) $\omega_\infty \gg \gamma$. We shall see that both inequalities are at least weakly satisfied in our results. With these assumptions $S(Q, \omega)$ can be easily divided into two contributions $S(Q, \omega) = S_{\text{sideband}}(Q, \omega) + S_{\text{central}}(Q, \omega)$ with

$$S_{\text{sideband}}(Q, \omega) = |F(Q)|^2 \frac{k_B T}{\pi \hbar} \frac{\Gamma^0}{(\omega_\infty^2 - \omega^2)^2 + (\omega \Gamma^0)^2}, \tag{10}$$

the familiar damped-harmonic-oscillator fluctuation spectrum. The additional term

$$S_{\text{central}}(Q, \omega) = |F(Q)|^2 \frac{k_B T}{\pi \hbar} \left(\frac{\delta^2}{\omega_0^2 \omega_\infty^2}\right) \frac{\gamma'}{\omega^2 + \gamma'^2} \tag{11}$$

is a Lorentzian centered about $\omega = 0$ and with width $\gamma' = \gamma(\omega_0/\omega_\infty)^2$. The integrated intensity is

$$\begin{aligned} I_{\text{total}}(Q) &= \int S(Q, \omega) d\omega \\ &= \int (S_{\text{sideband}}(Q, \omega) + S_{\text{central}}(Q, \omega)) d\omega \\ &= |F(Q)|^2 \frac{k_B T}{\pi \hbar} \left(\frac{1}{\omega_\infty^2} + \frac{\delta^2}{\omega_\infty^2 \omega_0^2}\right) \\ &= |F(Q)|^2 \frac{k_B T}{\pi \hbar} \frac{1}{\omega_0^2} \ . \end{aligned} \tag{12}$$

The fractional integrated intensity in the central peak is thus

$$\frac{I_{\text{central}}(Q)}{I_{\text{total}}(Q)} = \frac{(\delta^2/\omega_\infty^2 \omega_0^2)}{(1/\omega_0^2)} = \frac{\delta^2}{\omega_\infty^2} \ . \tag{13}$$

Suppose we couple with these relations "soft"-mode behavior, i.e., $\omega_\infty^2(s)$ gradually vanishing for a certain critical mode s as a phase transformation temperature T_M is approached from above. At high temperature ($\omega_\infty^2 \gg \delta^2$) there is a central component of width γ which is small but growing more rapidly (ω_∞^{-4} vs ω_∞^{-2}) than the phononlike sidebands. As $\omega_\infty^2 \to \delta^2$ this central component grows to dominate the spectrum, its intensity diverging and its width $\gamma' \to 0$ when $\omega_\infty^2 = \delta_s^2$. Note that it is this latter condition, i.e., $\omega_0^2(s) \to 0$ not $\omega_\infty^2 \to 0$, which marks the limit of stability of the high-temperature structure.

In order to relate the experimental observations to the discussion above we can proceed somewhat differently than in the similar study of soft-mode line shapes in $SrTiO_3$ and $KMnF_3$ by Shapiro *et al.*[30] In both of these latter cases a sizable central component was found only for modes with wave vectors very close to the critical wave vector q_s. Thus very little could be directly inferred about the q dependence of the central component, and very careful instrumental resolution corrections were necessary before a comparison of the experimental line shapes with Eq. (10) could be made. The small size of the Nb_3Sn sample limited the feasibility of a comparably detailed study, but fortunately (as shown in Fig. 8) the extension in reciprocal space of the central component is much larger than the

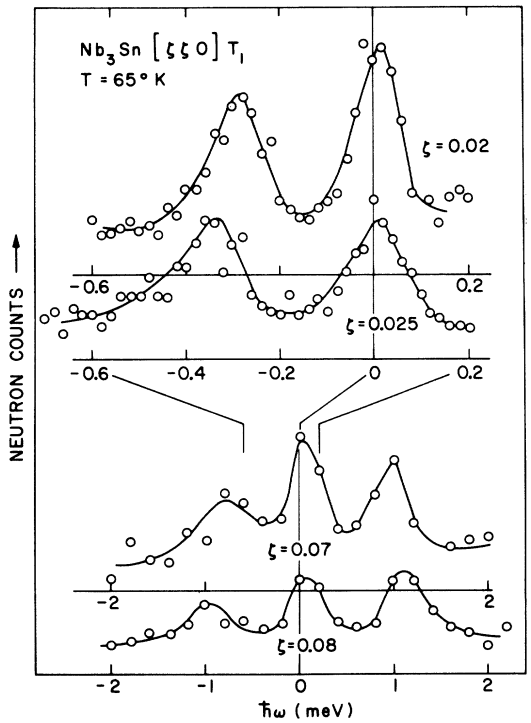

FIG. 9. Critical scattering spectral profile at 65°K for several values of momentum transfer, showing both the central component and phonon sideband(s). (Note the change in scale.)

corresponding q width of instrumental resolution. While the observed line shapes are still subject to considerable correction for finite energy resolution, within a reasonable first approximation the relative integrated intensities of the central and sideband components should be given directly from the experimental data.

Consider, for example, a series of experimental line shapes such as shown in Fig. 9 taken as a function of ζ along the soft $[\zeta\zeta 0]$ direction. Since from data such as this it is straightforward to obtain both the ratio $I_{\text{central}}(Q)/I_{\text{total}}(Q)$ and the value of ω_∞ (essentially the peak of the phonon sideband), Eq. (13) can be used to deduce a value for δ for each set of data. The results of such an analysis for not only the data shown in Fig. 9 but also for similar data taken at other temperatures is shown in Fig. 10. To be consistent with observations it is seen that δ must vary approximately linearly with q. This is consistent with the wave vector dependence predicted in the appendix and in fact follows from more basic continuity considerations as well. The observations admit at most a weak temperature dependence near T_M again in agreement with the mechanism considered in the Appendix.

Figure 11 demonstrates the agreement of the data with the other principal prediction of the phenom-

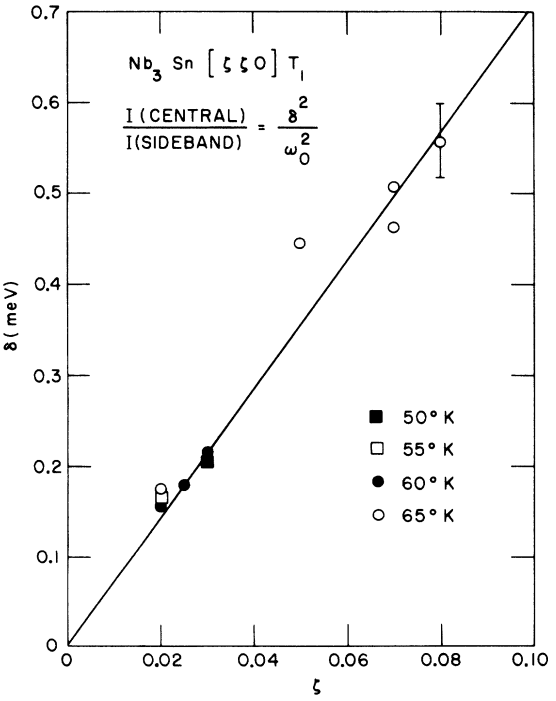

FIG. 10. Analysis of data similar to that shown in Fig. 9 establishing that the central component scattering amplitude $\delta(q)$ is linear in q and at most weakly temperature dependent.

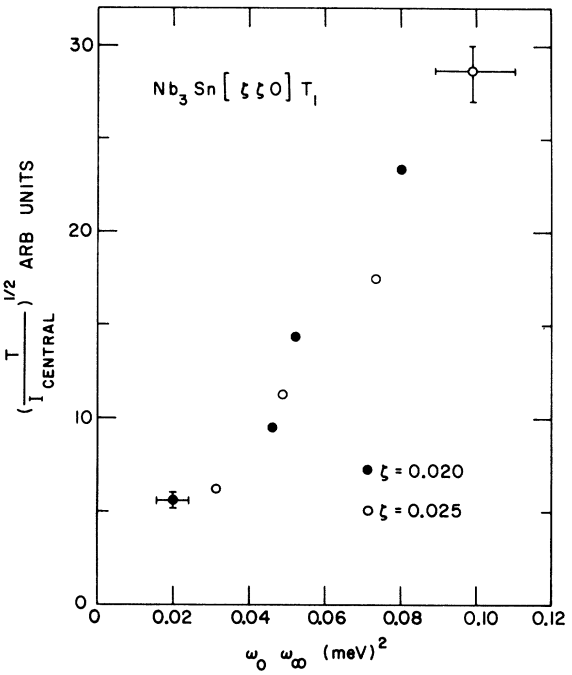

FIG. 11. Although the total critical scattering intensity diverges as T/ω_0^2, the intensity in the central component alone is proportional to $T/\omega_0^2\omega_\infty^2$.

enological theory, namely, that the central mode intensity grows not in proportion to the increasing intensity of the soft phonon sidebands ($\sim T/\omega_\infty^2$) but rather at the much faster rate ($\sim T/\omega_\infty^2\omega_0^2$). It is apparent that this relation is approximately obeyed over a reasonable range of temperatures for $[\zeta\zeta 0]T_1$ phonons with $\zeta \leq 0.025$. Here we have used a value of $(\delta/\zeta) = 7.1$ meV obtained from the analysis of Fig. 10.

There is one additional initially puzzling feature of our data which is resolved by our present understanding of the significance of the central mode. At room temperature the value of the $[\zeta\zeta 0]T_1$ phonon velocity derived from neutron measurements is essentially equal to that obtained by ultrasonic techniques.[8] However, as shown in Fig. 12 there is an increasing systematic discrepancy between the two types of measurements. We may suppose the ultrasonic frequency (40 MHz in this instance) to be negligibly small compared to the inverse relaxation time γ, so that one measures a collision-dominated velocity v_0. On the other hand, in accordance with usual practice, the frequencies from which the neutron data is derived are obtained from the phonon sidebands, i.e., they are the collision-free frequencies ω_∞, and thus lead to collision-free velocities, v_∞. Since

$$v_\infty^2 = \omega_\infty^2/q^2 = (\omega_0^2 + \delta^2)/q^2 \equiv v_0^2 + \lambda^2 , \qquad (14)$$

the value of $\lambda \equiv (\delta/q)$ determined previously may

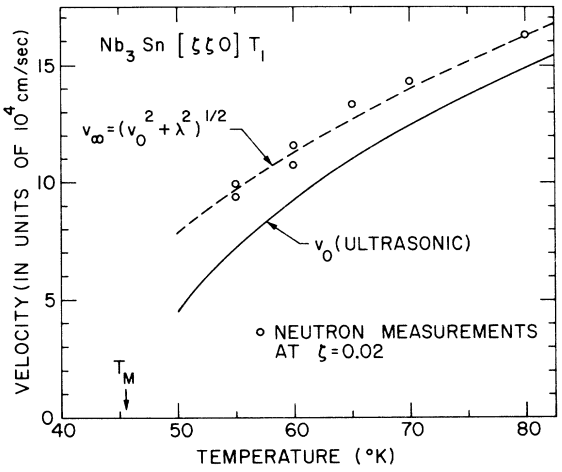

FIG. 12. $(\zeta\zeta 0)T_1$ phonon velocity determined by neutron scattering differs from ultrasonic velocities by an amount which is predictable from the amplitude of the central component.

now be used to convert the ultrasonic values of v_0 to v_∞. The results are in excellent agreement with the neutron results. At room temperature the calculated difference between v_0 and v_∞ is much reduced, again in agreement with observations.

Our discussion thus far has assumed from the outset that the scattering associated with the central mode is a part of the one-phonon response and is dynamical in nature, but with a narrow frequency response. However, in view of the fact that we have not succeeded in demonstrating experimentally an energy width, it is important to consider whether an alternative static mechanism could explain our observed central component. While it is true that the divergent intensity of the central component near T_M strongly suggests its dynamical origin, it is possible to imagine a plausible and somewhat trivial nondynamical mechanism involving scattering from static strain fields, which is at least in qualitative agreement with many of our observations. It is well known that point defects in a lattice will in general give rise to displacements of neighboring atoms from their equilibrium positions in the homogeneous impurity free crystal. These displacement fields cause diffuse scattering of x rays or neutrons sometimes known as Huang scattering. The magnitude of the displacement field about an impurity is calculated as a linear response to a force field $\vec{F}(\vec{r})$ which the impurity exerts on the undisplaced lattice. For our purposes it is convenient to Fourier transform the resulting displacements and express them in terms of a linear combination of phonon modes with wave vector q and branch index j. The amplitude of this impurity-induced phonon condensation $\langle Q_{jq}\rangle_{si}$ is easily shown in the harmonic approximation to be

$$\langle Q_{jq}\rangle_{si} = F_{jq}/\omega_{jq}^2 ,$$

where

$$F_{qj} = -N^{-1/2}\sum_{lk\alpha} F_{lk\alpha} M_k^{-1/2} e_{k\alpha}^*(qj)\, e^{-i\vec{q}\cdot\vec{l}}$$

is the projection of $\vec{F}(\vec{r}) \equiv \vec{F}_{lk}$ upon the phonon eigenvector $\vec{e}(q, j)$. The intensity of this static diffuse scattering can be calculated from the corresponding expression for the integrated phonon scattering under the same conditions by simply replacing $\langle Q_{qj}^2\rangle_{\text{thermal}}$ by $\langle Q_{qj}\rangle_{\text{impurity}}^2$.

$$[I_{qj}(\vec{Q})]_{\text{static impurity}} \propto |\langle Q_{qj}\rangle|_{si}^2 = \frac{|F_{qj}|^2}{\omega_{qj}^4} \qquad (15)$$

In normal materials the major contributions come from acoustic modes (because of ω_{qj}^{-4}) and the effect of impurity concentrations of $\sim 10^{-2}$ can easily be detected and studied against the thermal diffuse background by x-ray scattering.

Our interest is in applying Eq. (15) to a material with temperature-dependent mode frequencies $\omega_{q,s}(T)$ which become anomalously small near a structural transformation. If impurities are of the proper symmetry to produce nonvanishing $F_{q,s}$, there will be a central component in the scattering whose intensity grows more rapidly (ω_s^{-4}) than that of the collapsing phonon sidebands (ω_s^{-2}) as the transformation temperature is approached. Near $q=0$ for acoustic modes $F_{q,\text{ac}} \sim q$ so that $|F_{s,q}|^2$, just as $\delta_{q,s}^2$, would be proportional to q^2.

In spite of these obvious similarities, we do not believe that this impurity mechanism provides a satisfactory explanation of our observations. Although we have not until now made the distinction, it is clear that it is the low-frequency stiffness ω_0^2 which goes into Eq. (15) not ω_∞^2, *if there is a difference between the two quantities*. However, the static impurity mechanism acting alone provides no frequency-dependent terms to the phonon self-energy, so that $\omega_0^2 = \omega_\infty^2$ and $I_{\text{static}}(Q) \propto 1/\omega_\infty^4$. Our measurements as we have already shown closely follow $(1/\omega_0^2\omega_\infty^2)$, and there is a substantial difference between the two predictions especially near T_M. Simply put, ω_∞^2 (as obtained from the phonon sidebands) saturates near T_M while the central intensity continues to increase. Also the observed agreement with the discrepancy between the extrapolated long-wavelength acoustic velocities and our measurements and the magnitude of the central component would be entirely fortuitous for this (or for that matter any other) static description of the central component.

Although we conclude that the impurity effect proposed above is not a dominant one in our observations, it is certainly a plausible one for producing unusual line-shape effects near phonon instabilities and as such deserves further study. It should be clear from our brief formulation that the

basic considerations are by no means restricted to acoustic phonons, but are applicable for ferroelectric and "antiferroelectric" modes as well.

IV. INFLUENCE OF SUPERCONDUCTING ENERGY GAP UPON PHONON DAMPING

In addition to providing a plausible mechanism for the elastic instability of Nb_3Sn, Eq. (1) (or more specifically its imaginary part) predicts anomalously large phonon damping for $[\zeta\zeta 0]T_1$ modes due to electron-hole pair production. Schuster and Klose[36] have discussed in these terms the strongly temperature-dependent ultrasonic attenuation observed in V_3Si.[3] This phonon-damping mechanism is particularly interesting because it should be strongly modified by the appearance of an electronic energy gap, $2\Delta(T)$, in the superconducting phase.

In the superconducting phase it is useful to distinguish between two mechanisms for phonon damping. One is due to phonon scattering from thermally excited quasiparticles and vanishes as $T \to 0$. This has been extensively studied by ultrasonic-attenuation experiments.[37] The other process involves direct excitation by phonons of quasiparticles across the superconducting energy gap. This process is energetically impossible in ultrasound experiments since $\hbar\omega_{ac} \ll 2\Delta(T)$, except at $T \approx T_c$ where the contribution is negligible. But the process is important for higher-frequency phonons and is worthwhile to study because it sets in abruptly at a threshold phonon energy $\hbar\omega = 2\Delta(T)$. In principle it thus provides a means for direct determination of the temperature dependence and the anisotropy of the superconducting energy gap. A theoretical analysis of this superconducting-electron-pair breaking contribution to the attenuation of longitudinal acoustic phonons within the BCS model has been given by Bobetic.[38]

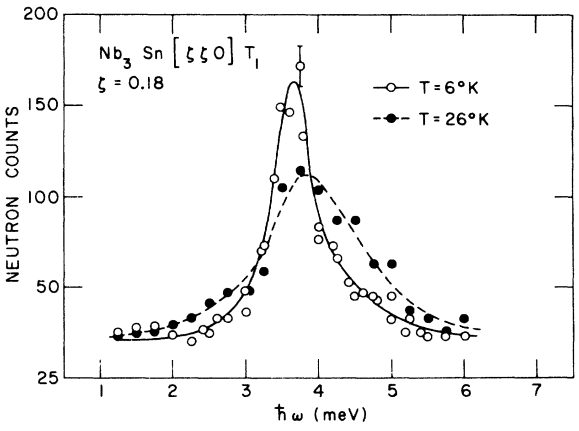

FIG. 13. Widths of low energy $[\zeta\zeta 0]T_1$ acoustic phonons broaden appreciably at temperatures near T_c, the superconducting transformation temperature. This figure shows the same phonon profile above and below $T_c = 18.0$ °K.

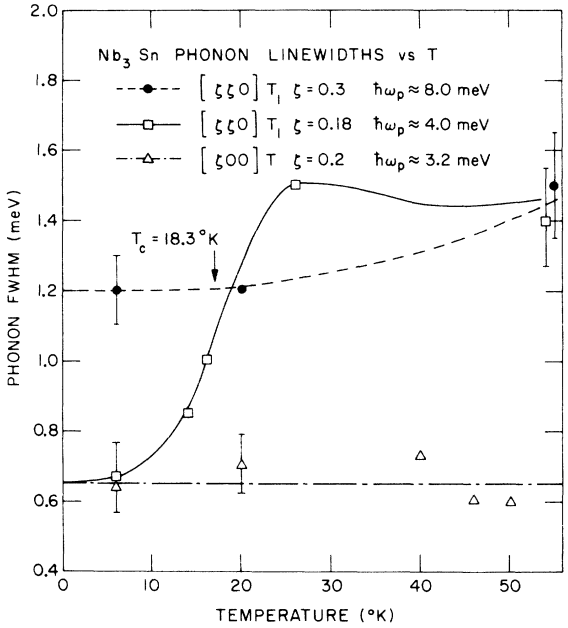

FIG. 14. Summary of TA-phonon linewidths near T_c. The unusually large $[\zeta\zeta 0]T_1$ linewidth is suppressed if the phonon energy $\hbar\omega_p$ is less than the superconducting gap energy $2\Delta(T)$.

Figure 13 shows an example of the change in the phonon line shape of a $[\zeta\zeta 0]T_1$ phonon observed in Nb_3Sn in the vicinity of the superconducting transformation temperature, $T_c = 18.0$ °K.[39] The intrinsic linewidth increases at least fourfold (≤ 0.3–1.4 meV) between 6 and 26 °K. [The low-temperature value represents an upper limit since the observed linewidth closely approximates the instrumental resolution width. The intrinsic widths were estimated using the Gaussian approximation, $(\Delta\omega^2)_{obs} = (\Delta\omega^2)_{res} + (\Delta\omega^2)_{intrinsic}$.] A similar rather sharp increase in the phonon damping occurs as the phonon energy is varied (by varying ζ) for $[\zeta\zeta 0]T_1$ phonons at a fixed low temperature. If this is identified with the onset of damping by quasiparticle production, the characteristic phonon energy at the onset can be estimated to be $\hbar\omega = 2\Delta(0) = 7 \pm 1$ meV $= (4.4 \pm 0.6) k_B T_c$. Those previous measurements thought to be reasonably representative of bulk Nb_3Sn have given values of $2\Delta(0)$ between 3.5 and 4.8 $k_B T_c$.[40]

A summary of the temperature dependence of the observed linewidth of various TA phonons is summarized in Fig. 14. $[\zeta\zeta 0]T_1$ phonon shown with energy $\hbar\omega < 7$ meV has narrow linewidth which increases rather abruptly at $T \leq T_c$ in qualitative agreement with theoretical expectation. [Indeed a reasonably good quantitative comparison of the phonon linewidths $2\Gamma(T)$ with the BCS model cal-

culations of Bobetic is found, even though such an explicit comparison is open to question.[40] The $[\zeta\zeta 0]T_1$ phonon with energy greater than $2\Delta(0)$ has a large and relatively temperature-independent linewidth reflecting the fact that it is able to decay by quasiparticle production at all temperatures.

Note from Fig. 14 that the $[\zeta 00]T$ phonon linewidths are small and temperature independent at low temperatures. This result is in agreement with a one-dimensional model of the d electrons, since a $[\zeta 00]$ shear motion produces no modulation of the interatomic separations within a given Nb chain. Also note in this connection that Klose and Schuster[41] predicted strong $[\zeta\zeta 0]$ transverse phonon-electron coupling and enhancement of T_c in the A-15 structure again using a one-dimensional model of the d electrons. It was not possible to obtain sufficiently high instrumental resolution to make a study of longitudinal phonon linewidths.

The superconducting energy gap selectively nullifies that part of the phonon linewidth γ_{ep} due to electron-phonon interaction. The relation of γ_{ep} to quantities of fundamental interest in superconductivity was recently pointed out by Allen,[42] who derived the following relation between $\langle\gamma_{ep}\rangle$ the average phonon linewidth and the electron-phonon coupling parameter λ which plays a prominent role in strong-coupling superconductors:

$$\langle\gamma_{ep}\rangle = \pi N(0)\langle\omega^2\rangle\lambda/6N ,$$

where $\langle\omega^2\rangle$ is the mean-square phonon frequency, $N(0)$ is the electronic density of states, and N is the number of atoms in the crystal. Applying this relation to Nb_3Sn one estimates $\langle\gamma_{ep}\rangle = 1.2$ meV.[14] Therefore, $[\zeta\zeta 0]T_1$ phonons ($\gamma_{ep} = 1.4$ meV) make a somewhat greater than average contribution to the phonon-mediated electron-electron interaction responsible for superconductivity, whereas $[\zeta 00]T$ phonons ($\gamma_{ep} \leq 0.3$ meV) contribute much less. These conclusions do not, however, take into account the recent conclusion of Allen[43] and Barisic,[44] that *very* soft phonons ($\omega \lesssim k_B T_c$) tend not to enhance but rather to destroy superconductivity.

There has been a recent emphasis in the literature on the importance of the phonon frequencies in optimizing the transformation temperature of a given class of superconductor and the extent to which this optimization process can be limited by structural instabilities. It is therefore interesting to verify that in Nb_3Sn, it is the same $[\zeta\zeta 0]T_1$ phonon branch in which the 45 °K structural instability develops which seems to make the largest contribution to the attractive electron interaction potential responsible for superconductivity.

ACKNOWLEDGMENTS

We thank J. J. Hanak and R. W. Cohen for permission to study the "RCA" Nb_3Sn sample, and to W. Rehwald for ultrasonic data prior to publication. We acknowledge helpful discussions with S. Barisic, R. W. Cohen, and especially with P. B. Allen and H. Schuster.

APPENDIX

We want to consider microscopic processes which give rise to phonon self-energies of the type proposed in Eq. (10). In particular, we examine the familiar anharmonic three-phonon scattering process with higher frequency thermal phonons, (acoustic) + (thermal) → (another thermal). We show that contributions from thermal phonons near topological critical points (i.e., $\nabla_q \Omega_{q\ (\text{thermal})} = 0$) are capable of producing the necessary structure in the acoustic phonon self-energy. In second-order perturbation theory, the imaginary self-energy which arises from real scattering process of this Raman type is given by

$$\mathrm{Im}\Pi_\mu(\omega) = \frac{-36\pi\Omega_\mu}{\hbar^2} \sum_{\mu_1\mu_2} |V_{\mu_1\mu_2-\mu}|^2 S_{12}(\omega) . \quad \text{(A1)}$$

$S_{12}(\omega)$, the imaginary part of a two phonon propagator represents the density of states into which the acoustic phonon with harmonic frequency Ω_μ can decay. $V_{\mu_1\mu_2-\mu}$ is the third-order term in expansion of the Hamiltonian in phonon coordinates. In lowest order one replaces the physical thermal phonons by their harmonic counterparts and obtains the familiar result

$$S_{12}(\omega) = (n_2 - n_1)[\delta(\Omega_1 - \Omega_2 - \omega) - \delta(\Omega_1 - \Omega_2 + \omega)] .$$

For small frequencies it is not permissible to neglect the finite lifetime of the thermal phonons themselves and a better approximation is obtained by replacing the harmonic spectral functions for the thermal phonons with approximate (Lorentzian) anharmonic ones. The result is

$$S_{12}(\omega) = n_1(n_1+1)\beta\omega \frac{1}{\pi}\left(\frac{\Gamma}{(\Delta-\omega)^2+\Gamma^2} + \frac{\Gamma}{(\Delta+\omega)^2+\Gamma^2}\right), \quad \text{(A2)}$$

where $\Delta = \Omega_1 - \Omega_2$ and $\Gamma = (\Gamma_1 + \Gamma_2)$ is the sum of the inverse lifetimes of the two thermal phonons. The factor $n_1(n_1+1)\beta\omega$ results from an expansion of $n_2 - n_1$ under the assumption that $\Omega_1, \Omega_2 \gg \omega$. Equations (A1) and (A2) form the basis of interpolation formulas between zero- and first-sound regimes. It is important to note that the final form of $\Pi_\mu(\omega)$ depends largely on the form of the dispersion relation for the thermal phonon states which are summed in Eq. (A1). Discussions to date have been based upon a Debye distribution of acoustic thermal phonons. This leads to structure in $\Pi_\mu(\omega)$ on a scale of Ω_μ which is insufficient to produce a sharp central peak although it does contribute to the first-sound response. We need terms which introduce structure into $\Pi_\mu(\omega)$ on the finer scale of $\omega \sim \Gamma \ll \Omega_\mu$,

and such structure may arise from nearly dispersionless thermal phonons such as occur in the neighborhood of critical points in the dispersion surface.

For simplicity assume a critical-point maximum or minimum locally of the form

$$\Omega_1 = \Omega_c + \tfrac{1}{2}\alpha\xi_1^2 , \tag{A3}$$

where $\vec{\xi}_1 = \vec{q}_1 - \vec{q}_c$ is the vector distance from the critical point. Assume for simplicity that this description holds within a sphere of radius ξ_M. Replacing the q sum in (A1) with an integral over the surface defined by (A3), which can be carried out in polar coordinates referred to the direction of the acoustic-phonon wave vector Q, we find

$$\begin{aligned}\mathrm{Im}\Pi_\mu(\omega) = {} & \frac{36\Omega_\mu}{\hbar^2}\, n_1(n_1+1)\beta\omega \left| V_{\mu_1-\mu_1-\mu}\right|^2 \frac{V}{8\pi^3} \\ & \times \int_0^{\xi_M} 4\pi\xi_1^2 d\xi_1 \frac{1}{\alpha Q\xi_1} \\ & \times \left[\tan^{-1}\left(\frac{\omega+\alpha Q\xi_1}{\Gamma}\right) - \tan^{-1}\left(\frac{\omega-\alpha Q\xi_1}{\Gamma}\right)\right].\end{aligned} \tag{A4}$$

We are concerned here only with that part of the integral which is sharply peaked about $\omega = 0$ which we can insure by replacing the upper limit ξ_M by ξ_c such that $\alpha Q\xi_c \equiv \Gamma$. (The contributions from larger values of ξ_1, being more slowly varying with frequency, can be combined with other scattering processes into a frequency independent damping Γ_0.) Then it is permissible to expand the $\tan^{-1}$ in powers of $(\alpha Q\xi_1/\Gamma)$ after which the integral becomes proportional to $\frac{8}{3}\xi_c^3$, the effective volume of phase space about the critical point. It is also convenient for numerical estimates to introduce the Grüneisen approximation

$$\left| V_{\mu_1-\mu_1-\mu}\right|^2 = \gamma^2\hbar^3\Omega_1^2\Omega_\mu/2NMv^2 ,$$

where M is the mass of a unit cell and v is an average acoustic-phonon frequency. Equation (A4) can then be cast in a form

$$\mathrm{Im}\Pi_\mu(\omega) = \lambda^2 Q^2 \frac{\omega\Gamma}{\omega^2+\Gamma^2} , \tag{A5}$$

with

$$\begin{aligned}\lambda^2 &= 36\gamma^2(\xi_c/\xi_D)^3\, n_1(n_1+1)\beta\Omega_1(\hbar\Omega_1/M) \\ &= 36\gamma^2 k_B T(\xi_c/\xi_D)^3, \text{ if } \hbar\Omega_1 \gg k_B T\end{aligned} \tag{A6}$$

where ξ_D is the Debye wave vector $(6\Pi^2N/V)^{1/3}$ so that $(\xi_c/\xi_D)^3$ is the *fractional* volume of q space about the critical point effective in contributing to the low-frequency self-energy. For Q smaller than a critical size (which depends upon the magnitude of Γ) the full dimension of the critical region ξ_M contributes to the narrow central component

$$\xi_c = \xi_M, \text{ for } Q \le Q_c \equiv (\Gamma/\alpha\xi_M) \tag{A7a}$$

and $\Pi_\mu(Q)$ is proportional to Q^2. For larger values of Q,

$$\xi_c = (\Gamma/\alpha Q), \text{ for } Q > Q_c \tag{A7b}$$

and $\Pi_\mu(Q)$ falls off as $1/Q$.

The contribution to the real self energy which corresponds to Eq. (A5) is given exactly by the dispersion relation

$$\mathrm{Re}\Pi_\mu(\omega) = \frac{1}{\pi}\int_{-\infty}^{\infty} \frac{\mathrm{Im}\Pi_\mu(\omega')}{\omega'-\omega}\, d\omega'$$

and is

$$\mathrm{Re}\Pi_\mu(\omega) = \lambda^2 Q^2 \frac{\Gamma^2}{\omega^2+\Gamma^2} . \tag{A8}$$

Q_c depends both upon the dispersion and damping of phonons near the critical points but for typical cases it is expected that $\frac{1}{10} < Q_c/\xi_M < 1$. To get an estimate of the strength of the renormalization take $\gamma = 1$, $M = 100$ amu and $\hbar\Omega_1/k \cong T = 100\ ^\circ\mathrm{K}$. Then we find $\lambda^2 = 3.3\times10^9(\xi_c/\xi_D)^3$ (cm/sec)^2 so that a critical volume fraction (from all critical points) of the order of 10^{-2} is sufficient to give λ (the maximum renormalization of the phonon velocity) $\sim 5\times10^3$ cm/sec $\sim \frac{1}{100}$ (typical sound velocity). This estimate of λ represents a small but non-negligible contribution in normal materials and is smaller by ~ 10 than is necessary to explain the magnitude of the central component in Nb_3Sn. There is however good reason to suppose that the Grüneisen parameter γ_s for the "soft" modes in Nb_3Sn is substantially greater than unity. From measurements of pressure-dependent shear modulus at higher temperatures, Carcia *et al.* deduce $\gamma_s \sim 5.5$ near the transformation temperature $T_M = 20\ ^\circ\mathrm{K}$ in V_3Si. If a value of γ_s of this magnitude were applicable in Nb_3Sn the mechanism appears to be a feasible one.

There are however some features that are not easily understood from the above considerations. The enhanced-mode Grüneisen parameter required for adequate interaction strength would in this model enhance equally contributions from all thermal phonons to the soft-mode self-energy. Most such contributions are not sharply peaked near $\omega = 0$, yet the experimental difference between zero- and first-sound velocities is quantitatively accounted for by this sharply peaked component above. Also if, as is the case for V_3Si, the enhancement of γ_s is strongly temperature dependent this should be reflected in the temperature dependence of the coupling parameter γ^2. A temperature-independent γ^2 suffices to fit the experimental data. It is possible that some insight into these problems could be obtained from a more sophisticated theoretical treatment. It does not appear that so-called vertex corrections will appreciably alter these results al-

though they are very important for longitudinal phonons.[45] Nevertheless, it is highly doubtful that second-order perturbation theory works quantitatively near T_M. In particular, perhaps an important group of interacting phonons are those near the critical point which develops on the soft branch itself as $v_s \to 0$. Then no clear distinction between soft acoustic and thermal phonons is possible, and some self-consistent treatment of all modes on an equal footing would seem to be required.

Note added in proof. In a recent publication [Solid State Commun. 11, 1361 (1972)], B. Horovitz, H. Gutfreund, and M. Weger discuss the nature of the Kohn anomaly in systems with planar Fermi surfaces, taking care to include the effects from imaginary self-energy terms. W. Dieterich has recently studied the effect of d-electron scattering on the Grüneisen constants of $A15$-compounds [*Z. Phys.* 254, 464 (1972)], and finds that the effects are large and temperature dependent.

---

*Work performed under the auspices of the U.S. Atomic Energy Commission.

[1]See, for example, B. T. Matthias, Science **156**, 645 (1967).
[2]B. W. Batterman and C. S. Barrett, Phys. Rev. Lett. **13**, 390 (1964); Phys. Rev. **145**, 296 (1966).
[3]L. R. Testardi and T. B. Bateman, Phys. Rev. **154**, 402 (1967).
[4]K. R. Keller and J. J. Hanak, Phys. Rev. **154**, 628 (1967).
[5]R. Mailfort, B. W. Batterman, and J. J. Hanak, Phys. Lett. **24**, 315 (1967).
[6]L. J. Vieland, R. W. Cohen, and W. Rehwald, Phys. Rev. Lett. **26**, 373 (1971).
[7]L. J. Vieland, J. Phys. Chem. Solids **31**, 1449 (1970).
[8]W. Rehwald, M. Rayl, R. W. Cohen, and G. D. Cody, Phys. Rev. B **6**, 363 (1972).
[9]W. Rehwald, Phys. Lett. A **27A**, 287 (1968).
[10]P. F. Carcia, G. R. Barsch, and L. R. Testardi, Phys. Rev. Lett. 27, 944 (1971).
[11]J. Labbé and J. Friedel, J. Phys. (Paris) **27**, 153 (1966); J. Phys. (Paris) **27**, 303 (1966); J. Phys. (Paris) **27**, 708 (1966).
[12]J. Labbé, Phys. Rev. **149**, 246 (1966); Phys. Rev. **158**, 647 (1967); Phys. Rev. **158**, 655 (1967); Phys. Rev. **172**, 451 (1968).
[13]S. Barisic and J. Labbé, J. Phys. Chem. Solids **28**, 2477 (1967).
[14]J. Labbé, S. Barisic, and J. Friedel, Phys. Rev. Lett. **19**, 1039 (1967).
[15]R. W. Cohen, G. D. Cody, and J. J. Halloran, Phys. Rev. Lett. **19**, 840 (1967).
[16]E. Pytte, Phys. Rev. Lett. **25**, 1176 (1970); Phys. Rev. B **4**, 1094 (1971).
[17]L. R. Testardi, J. E. Kunstler, H. J. Levenstein, J. P. Maita, and J. H. Wernick, Phys. Rev. B **3**, 107 (1971).
[18]L. J. Vieland and A. W. Wickland, Phys. Rev. **166**, 425 (1968).
[19]G. Shirane, J. D. Axe, and R. J. Birgeneau, Solid State Commun. **9**, 397 (1971).
[20]G. Shirane and J. D. Axe, Phys. Rev. B **4**, 2957 (1971).
[21]L. J. Sham, Phys. Rev. Lett. **27**, 1725 (1971).
[22]G. Shirane and J. D. Axe, Phys. Rev. Lett. **27**, 1803 (1971).
[23]J. J. Hanak and H. S. Berman, J. Phys. Chem. Solids **28**, 249 (1967).
[24]T. Riste and K. Otnes, Nucl. Instrum. Methods **75**, 197 (1969); G. Shirane and V. J. Minkiewicz, Nucl. Instrum. Methods **89**, 109 (1970).
[25]W. Dieterich and H. Schuster, Phys. Lett. A **35**, 48 (1971).
[26]E. J. Woll and W. Kohn, Phys. Rev. **126**, 1693 (1962).
[27]S. Barisic, Solid State Commun. **9**, 1507 (1971).
[28]S. Berko and M. Weger, Phys. Rev. Lett. **24**, 55 (1970).
[29]T. Riste, E. J. Samuelsen, K. Otnes, and J. Feder, Solid State Commun. **9**, 1455 (1971).
[30]S. M. Shapiro, J. D. Axe, G. Shirane, and T. Riste, Phys. Rev. B **6**, 4332 (1972).
[31]Feder has argued that nonlinear coupling of the order parameter with temperature give rise to higher-order differences between adiabatic and isothermal response even if $d\eta/dT = 0$ [J. Feder, Solid State Commun. **9**, 2021 (1971)].
[32]R. D. Mountain, J. Res. Natl. Bur. Stand. (U.S.) A **70**, 207 (1966).
[33]R. A. Cowley, J. Phys. Soc. Jap. Suppl. **28**, S239 (1970).
[34]See, for example, P. C. Kwok, in *Solid State Physics*, edited by F. Seitz and D. Turnbull (Academic, New York, 1967), Vol. 20, p. 233.
[35]L. J. Sham, Phys. Rev. **156**, 494 (1967); G. Niklasson, Ann. Phys. (N.Y.) **59**, 263 (1970); R. Klein and R. K. Wehner, Phys. Kondens. Mater. **8**, 141 (1968); Phys. Kondens. Mater. **10**, 1 (1969).
[36]H. Schuster and W. Klose, Phys. Lett. A **34**, 152 (1971).
[37]For a compendium of such measurements, see L. M. Falicov and D. H. Douglass, in *Progress in Low Temperature Physics*, edited by J. C. Gorter (North-Holland, Amsterdam, 1964), pp. 97–189.
[38]V. M. Bobetic, Phys. Rev. **136**, A1535 (1964).
[39]We continue to use cubic notation in the tetragonal state. This is consistent with our failure to discern experimentally the cubic degeneracies of the phonon energies. Likewise, we believe our linewidth measurements are unaffected by domain-wall motion, although this is thought to be a major problem at ultrasonic frequencies.
[40]L. Y. L. Shen, Phys. Rev. Lett. **29**, 1082 (1972); D. R. Bosomworth and G. W. Cullen, Phys. Rev. **160**, 364 (1967); L. J. Vieland and A. W. Wicklund, Phys. Rev. **166**, 424 (1968).
[41]These calculations assume longitudinal interacting with a spherical Fermi surface. Transverse phonons have the complication of transverse magnetic fields which become screened by the Meissner effect. For the nonspherical Fermi surface, it is not possible to excite minimum-energy quasiparticles for all $q \leq 2k_F$. Thus the value $2\Delta(0) = 7 \pm 1$ meV represents strictly an upper limit. This point was brought to our attention by H. Schuster (private communication), who will shortly publish a further analysis of the interpretation of our data as it is influenced by Fermi-surface geometry.
[42]P. B. Allen, Phys. Rev. B **6**, 2577 (1972).
[43]P. B. Allen, Bull. Am. Phys. Soc. **18**, 76 (1973).
[44]S. Barisic, Phys. Rev. B **5**, 932 (1972).
[45]G. Niklasson, in *Proceedings of 1971 Rennes Conference on Phonons* (Flammarion, Paris, 1972).